LBL-10937 c.2
Preprint

Lawrence Berkeley Laboratory
UNIVERSITY OF CALIFORNIA

Materials & Molecular Research Division

Submitted to the Journal of the Electrochemical Society

THE KINETICS OF THE O_2/CO_2 REACTION IN MOLTEN CARBONATE: REACTION ORDERS FOR O_2 AND CO_2 ON NiO

Jack Winnick and Philip N. Ross, Jr.

May 1980

RECEIVED
LAWRENCE
BERKELEY LABORATORY

JUL 9 1980

LIBRARY AND
DOCUMENTS SECTION

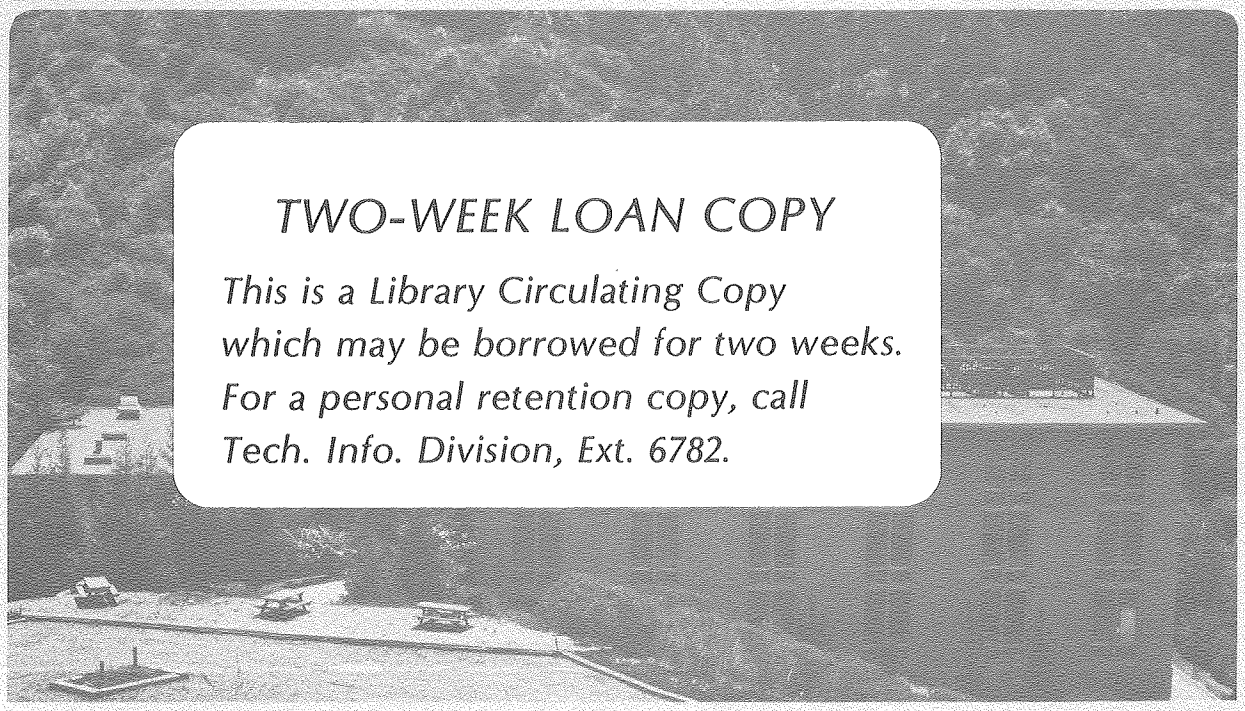

TWO-WEEK LOAN COPY

This is a Library Circulating Copy which may be borrowed for two weeks. For a personal retention copy, call Tech. Info. Division, Ext. 6782.

LBL-10937 c.2

Prepared for the U.S. Department of Energy under Contract W-7405-ENG-48

DISCLAIMER

This document was prepared as an account of work sponsored by the United States Government. While this document is believed to contain correct information, neither the United States Government nor any agency thereof, nor the Regents of the University of California, nor any of their employees, makes any warranty, express or implied, or assumes any legal responsibility for the accuracy, completeness, or usefulness of any information, apparatus, product, or process disclosed, or represents that its use would not infringe privately owned rights. Reference herein to any specific commercial product, process, or service by its trade name, trademark, manufacturer, or otherwise, does not necessarily constitute or imply its endorsement, recommendation, or favoring by the United States Government or any agency thereof, or the Regents of the University of California. The views and opinions of authors expressed herein do not necessarily state or reflect those of the United States Government or any agency thereof or the Regents of the University of California.

THE KINETICS OF THE O_2/CO_2 REACTION IN MOLTEN CARBONATE: REACTION ORDERS FOR O_2 AND CO_2 ON NiO

Jack Winnick
Department of Chemical Engineering
Georgia Institute of Technology
Atlanta, Georgia 30332

and

Philip N. Ross, Jr.
Lawrence Berkeley Laboratory
Materials and Molecular Research Division
University of California
Berkeley, California 94720

LBL-10937

INTRODUCTION

The molten carbonate fuel cell is undergoing extensive research and development[1-3] as a potential option for converting synthesis gas to electric power. In these cells a fuel gas containing principally hydrogen and carbon monoxide is electrochemically oxidized in the fuel cell anode

$$H_2 + CO_3^{2-} \rightarrow H_2O + CO_2 + 2e^- \qquad (1)$$

$$CO + CO_3^{2-} \rightarrow 2CO_2 + 2e^-$$

The carbon dioxide produced is recycled to the air intake for the cathode to form the gas mixture that is electrochemically reduced,

$$CO_2 + \frac{1}{2} O_2 + 2e^- \rightarrow CO_3^{2-} \qquad (2)$$

This process is somewhat similar to that which occurs in the aqueous alkaline electrolysis cell used by NASA as a CO_2 concentrator[4-6]. Ambient levels of CO_2 are removed at the cathode to be rejected at high concentration of the anode. A molten carbonate electrolyte cell also has the promise of use as a CO_2 concentrator, either with a reducing gas at the anode or in an electrolysis mode. In the latter case, application of an external potential produces a concentration gradient across the cell, the cathodic reaction being the evolution of CO_2 from the carbonate melt,

$$CO_3^{2-} \rightarrow CO_2 + \frac{1}{2} O_2 + 2e^-$$

Recent work on molten carbonate cells has focused on either the kinetics in free electrolyte on noble electrodes[7] or performance

characteristics of subscale commercial cells with paste electrolyte and porous nickel electrodes[2-3]. Development of these cells as gas concentrators requires knowledge of the behavior under both anodic and cathodic polarization with very low CO_2 partial pressures. Fundamentally, observation of the kinetic reaction orders is an essential step in the evaluation mechanistic sequences proposed for the O_2/CO_2 reaction.

The basic experimental approach we have used in this work is similar to that used in the classic experiments of Broers and Katelaar[8]. Here we employed paste electrolytes and nickel sinter electrodes. The advantage of this apparatus over a free-electrolyte cell is that the gas diffusion properties are such that the limiting currents are very high and a region of overpotential exists where kinetically controlled currents can be measured if the exchange currents are below ca. 1 mA/cm^2[9]. The disadvantage of such cells is that the total electrode-electrolyte interfacial area is unknown.

We have used a two-step approach to the determination of reaction orders. First, exchange currents at various P_{CO_2} and P_{O_2} were measured using the low polarization method. We assume a steady-state current-voltage relationship of the form

$$I = I_o \left[\exp\,(\alpha_+ F\eta/RT) - \exp\,(-\alpha_- F\eta/RT)\right] \qquad (3)$$

where $\eta = E-E_o$, α_+ is the anodic transfer coefficient, α_- the cathodic transfer coefficient ($\alpha_+ + \alpha_- = 2$). For $\eta \ll \alpha RT/F$, equation (3) simplifies to

$$I \doteq (2FI_o/RT)\,\eta$$

so that $I_o = (RT/2F)(\partial I/\partial \eta)_{T,P}$. The reaction orders can be obtained from the partial pressure dependence of I_o and the values of the transfer coefficient α_+ and α_-. Let

$$\left(\frac{\partial \log I_o}{\partial \log P_{CO_2}}\right)_T = m \tag{4}$$

$$\left(\frac{\partial \log I_o}{\partial \log P_{O_2}}\right)_T = n \tag{5}$$

then the reaction orders for the anodic (I_+) and cathodic (I_-) partial currents are, therefore,

$$\left(\frac{\partial \log I_\pm}{\partial \log P_{CO_2}}\right)_T = \begin{cases} m - 1 + (\alpha_-/2) \\ m + (\alpha_-/2) \end{cases} \tag{6}$$

$$\left(\frac{\partial \log I_\pm}{\partial \log P_{O_2}}\right)_T = \begin{cases} n - 1/2 + (\alpha_-/4) \\ n + (\alpha_-/4) \end{cases} \tag{7}$$

Second, the transfer coefficients were obtained from the slope of the Allen-Hickling plot

$$\mathrm{Ln}\left[I/\{\exp(2F\eta/RT) - 1\}\right] = \mathrm{Ln}I_o - (\alpha_- F\eta/RT) \tag{8}$$

for current densities low enough so that concentration polarization within the electrode can be neglected.

APPARATUS AND PROCEDURE

We assembled a molten carbonate test cell using paste electrolyte tiles and porous nickel electrodes typical of those used in

current subscale molten carbonate cells. The cell was comprised of two housings of 316 stainless steel which hold the electrolyte tile between them. The electrodes, made of porous nickel, were 0.07 cm in thickness and 1.9 cm in diameter. They fitted snugly in the center of the cavity, in firm contact with the gas distributors. (See Fig. 1.) The faces of the housings were aluminized to provide a wet-seal against the tile upon melting of the carbonate. The upper housing had a 0.5 cm hole drilled through for the reference electrode, which was a gold flag suspended in the eutectic melt, as in Fig. 2. The noble gas mixture (67% CO_2, 33% O_2) was bubbled slowly through the inner alumina tube past the electrode and then out through the center tube. A small hole in the bottom of the outer tube allowed communication between the free electrolyte in the tube and that in the tile. The upper housing had a well in which was placed an iron-constantan thermocouple, sheathed in a stainless tube and mounted with a standard fitting. When assembled, the cell was mounted on a ceramic block, held in place with steel guides and placed inside a furnace made of two clam-shell heaters. The gas inlet line, of stainless tubing, passed around the outside of the heater, allowing the gas to be pre-heated before entry into the cell. The outlet line, also of stainless, led straight out of the furnace. The furnace was insulated with transite panels and fibrous zirconia felt. The entire apparatus was mounted in a steel frame and a pneumatic cylinder applied pressure to the top of the upper housing to assure firm contact between cell components.

The gases were calibrated mixtures purchased from Matheson. Fifteen binary combinations were used from the matrix 0.5, 1, 10, 20,

50% CO_2: 1, 19 50% O_2, the balance N_2 in every case. The noble gas mixture 67% CO_2/33% O_2 was used as the reference gas.

The experiments were begun by assembling the cell with an electrolyte tile supplied by Argonne National Laboratory. The composition by weight of this tile is 25.6% Li_2CO_2, 29.4% K_2CO_3 and 45.0% $LiAlO_2$. The porous electrodes were fabricated by Gould for use in molten carbonate fuel cells and were pure nickel when the cell was assembled. The physical characteristics of these electrodes are given in Table 1. At startup, the cell was heated slowly while oxidant gases continually flowed over both electrodes. About five hours were necessary to bring the cell to 600°C. The cell was left in this open-circuit condition for 30-50 hrs. before experiments were begun to assure complete conversion of the electrodes to NiO.

Measurements were made only of the steady-state polarization of the top electrode using a Princeton Applied Research Potentiostat/Galvanostat (Model 371) in the galvanostatic mode. The gas flow to the top electrode was increased until no change in polarization was seen. The voltage reading was taken when apparent steady-state was reached although some fluctuation was still seen. A current-interruption technique was occasionally employed to measure the IR drop between reference and top electrode. This loss averaged about 3 mV at 100 mA, as measured on an oscilloscope (Tektronix 5111) and was linear over the range studied. This yields a specific conductivity of 2.1 $(\text{ohm cm})^{-1}$ for the 0.18 cm thick tile. The current was increased step-wise until the potential was about -0.5V (all potentials are relative to the 67% CO_2/33% O_2 reference electrode). Larger polarizations were avoided because, in a sacrificial experiment, cyclic voltammetry disclosed that the reduction of NiO to Ni occurred at about

-0.6V and cycling the electrode through this potential region irreversibly changed the electrolyte/porous electrode structure.

RESULTS

The use of very low polarizations and the linear form of equation (3) to measure exchange current requires the absence of interfering reactions near the rest potential of the system, i.e. the observed rest potential is not a mixed potential. The rest potentials we observed were within ±2 mV of the theoretical open circuit calculated from the Nernst equation

$$E = E_o + \frac{RT}{2F} \text{Ln } P_{CO_2} P_{O_2}^{1/2} \qquad (9)$$

After anodic or cathodic polarization, the cell returned quickly to the starting rest potential. These observations indicated the only faradaic processes occurring at a measureable rate near the rest potential is the O_2/CO_2 reaction. Typical current-voltage curves in the very low polarization region are shown in Fig. 3. These curves were reasonably linear and showed clearly that the partial pressure dependence of the exchange current, which is proportional to the slope of these lines, is very nearly zero. More than 100 sets of curves were obtained with varying gas composition and temperature. The resulting correlation was

$$I_o = (1.5\text{x}10^2)\ P_{CO_2}^{0}\ P_{O_2}^{0.5} \exp\left[-6\text{x}10^3/(T+273)\right] \qquad (10)$$

where I_o is A/cm^2 for T = 550-750°C and partial pressures of 0.1-0.5 atm. We can report only the exchange current density per <u>external</u>

area of electrode, since the internal area of the electrode contacted by electrolyte is not known. If all of the internal area were contacted, then about 100 cm^2 of NiO is available per cm^2 external area. At 700°C, this would mean an i_o of about 1.4 mA/cm^2 for 20% CO_2/20% O_2, about the same as that found by Appleby and Nicholson for smooth Au in Li/K eutectic melt[10].

The second step necessary for determining reaction orders according to equations (6) and (7) is the measurement of the cathodic transfer coefficient, α_-. The current-voltage behavior of these electrodes at polarizations ca. RT/F was typically like those in Fig. 4; no reaction limiting current was observed either anodically or cathodically, nor was a cathodic diffusion limiting current observed above -0.6V, where the NiO undergoes reduction to Ni. At current densities an order of magnitude below the diffusion limiting current, the currents are predominantly kinetically controlled. Typical Allen-Hickling plots for cathodic polarizations to 2 RT/F are shown in Fig. 5. According to equation (8), the intercept is just LnI_o, which Fig. 5 shows corresponds to $I_o \doteq 150$ mA (53.5 mA/cm^2 external), in good agreement with the Fig. 3 values. The average values found from analysis of ca. 100 polarization curves were 0.5 ± 0.1 for α_-, 1.6 ± 0.1 for α_+. Fig. 5 also shows the characteristic effect of CO_2 partial pressure on both I_o and α_- and, as in Fig. 3, the exchange current is essentially zero-order in CO_2 pressure. From equations (6) and (7), the reaction orders are, therefore,

$$\left(\frac{\partial \log I_{\pm}}{\partial \log P_{CO_2}}\right)_T = \begin{cases} -3/4 \\ +1/4 \end{cases} \tag{11}$$

$$\left(\frac{\partial \log I_{\pm}}{\partial \log P_{O_2}}\right)_T = \begin{cases} +1/8 \\ +5/8 \end{cases} \tag{12}$$

DISCUSSION

It should be emphasized that the reaction orders given by equations (11) and (12) represent only apparent reaction orders, and not necessarily the true kinetic reaction orders. The distinction arises because the values of the transfer coefficient (α_-) were determined using porous electrodes, and the possible effects of diffusion on the polarization behavior of these electrodes must either be accounted for or eliminated experimentally. Modelling studies[9] on Ni sinter electrodes like those used here have indicated that diffusion polarization is not significant for total polarizations ca. RT/F if the carbonate melt wets the electrode in an optimal fashion. The very high limiting currents observed with these electrodes (as in Fig. 4) indicate that the ideal thin-meniscus structure was approached with this cell configuration, and that polarization behavior observed here was essentially kinetically controlled. Independent studies[11] utilizing non-porous electrodes and applying transient techniques have indicated the transfer coefficient α_- is 0.6 ± 0.05, close to that found here. However, while there is some support for a claim that the reaction orders found in this work are the kinetic orders, the determination is certainly not definitive. More properly, one should regard

these reaction orders as representative of the polarization behavior of the paste electrolyte-Ni sinter electrode technology represented by our apparatus. As such, they are useful for systems analysis and for the design of large scale hardware based on this representative technology.

The cathodic reaction, of primary interest for fuel cell application, has a low but finite order in CO_2 pressure and the power density of the cell at constant voltage will increase with increasing CO_2 pressure. However, increasing CO_2 partial pressure decreases O_2 pressure, and since the reaction order for O_2 is higher than that for CO_2, this will result in a power density function that has an optimum CO_2/O_2 ratio. For an oxidant gas where $P_{CO_2} + P_{O_2}$ = const., it can be shown that the optimum $CO_2:O_2$ ratio is 2:5.

The reaction orders in CO_2 are ideally suited to the operation of this cell as a gas concentrator. In this application, CO_2 is removed from a $CO_2.O_2$ mixture with very low (e.g. 0.005 atm) CO_2 partial pressure by cathodic reduction to CO_3^{2-}, and transported by anodic evolution to a carrier gas stream where the CO_2 pressure is relatively high. The cathodic reaction has a low order in CO_2, so that the kinetics for CO_2 reduction are high even at very low CO_2 partial pressure.

ACKNOWLEDGMENTS

This work was done at the Lawrence Berkeley Laboratory with financial support from the National Aeronautics and Space Administration (Research Contract NSG-2193) and the U. S. Department of Energy (Contract W-7405-ENG-48). We thank Dr. Kim Kinoshita of the Argonne National Laboratory for supplying the electrolyte tiles and Mr. Charles Iacovangelo of the General Electric Research Center for valuable assistance in design of the cell.

REFERENCES

1. Argonne National Laboratory, Contract No. W-31-109-ENG-38, Report No. ANL78-71, August 1978.

2. United Technologies Corporation, Research Project 114-2, Report EM-956, December 1978.

3. Institute of Gas Technology, Project 9105, Final Report, April 1979.

4. J. Winnick and C. H. Lin, I. and E.C. Proc. Des. Dev., 13, 59 (1974).

5. C. H. Lin and J. Winnick, I. and E.C. Proc. Des. Dev., 13, 63 (1974).

6. C. H. Lin and J. Winnick, I. and E.C. Proc. Des. Dev., 13, 261 (1974).

7. A. J. Appleby and S. B. Nicholson, J. Electroanal. Chem., 53, 105 (1974), J. Electroanal. Chem., 83, 309 (1977).

8. G. Broers and J. Ketelaar, in "Fuel Cells", ed. G. Young, Reinhold Publishing, New York, 1960, pp. 78-94.

9. J. Selman, H. Mann, V. Sampath and L. Marianowoki, in Proceedings of Symp on Electrode Materials and Processes for Energy Conversion and Storage, The Electrochemical Society, Vol. 77-6, 1977, pp. 656-681.

10. A. J. Appleby and S. B. Nicholson, to be published in J. Electroanal. Chem., 1980.

11. J. Winnick and P. N. Ross, Jr., Extended Abstracts, Vol. 80-2, The Electrochemical Society, Princeton, New Jersey, 1980; to be published in J. Electrochem. Soc.

TABLE 1

Physical Characteristics of Ni Sinter Electrodes

Mean Pore Size, μm	9
Pore Size Distribution (80%), μm	3 to 16
Porosity	77%
BET Surface Area	0.15 m^2/g
BET Area After Oxidation	0.20 m^2/g

FIGURE CAPTIONS

Figure 1 - Schematic diagram of the electrolysis cell assembly, XBL 805-777.

Figure 2 - Schematic diagram of the reference electrode. XBL 805-776.

Figure 3 - Polarization curves near the rest potential as a function of CO_2 pressure. XBL 805-780A.

Figure 4 - Cathodic current-voltage behavior for porous Ni electrodes. XBL 805-781.

Figure 5 - Allen-Hickling plots of cathodic polarization data for porous Ni electrodes as a function of CO_2 partial pressure. XBL 805-782.

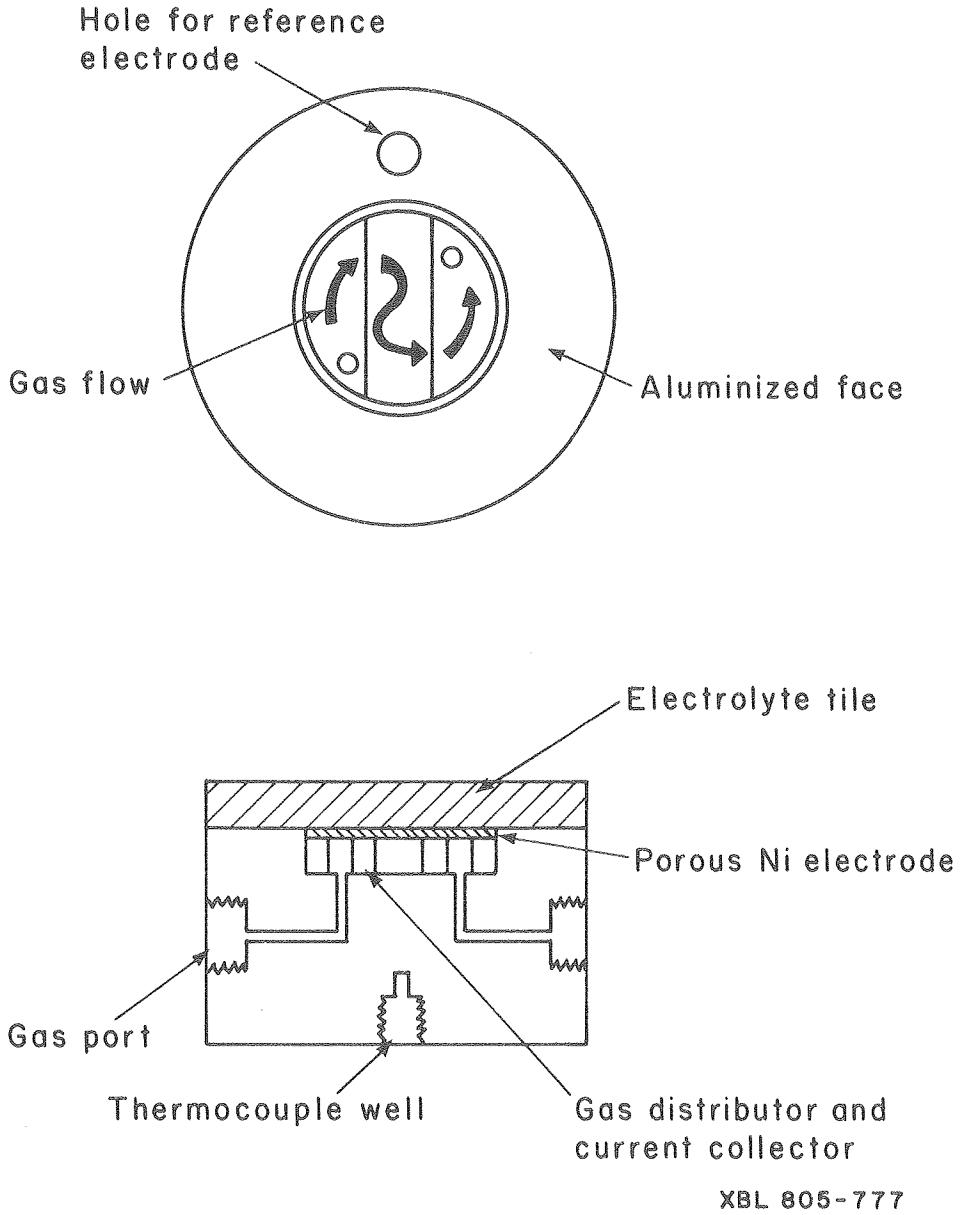
Hole for reference electrode
Gas flow
Aluminized face
Electrolyte tile
Porous Ni electrode
Gas port
Thermocouple well
Gas distributor and current collector
XBL 805-777

FIGURE 1

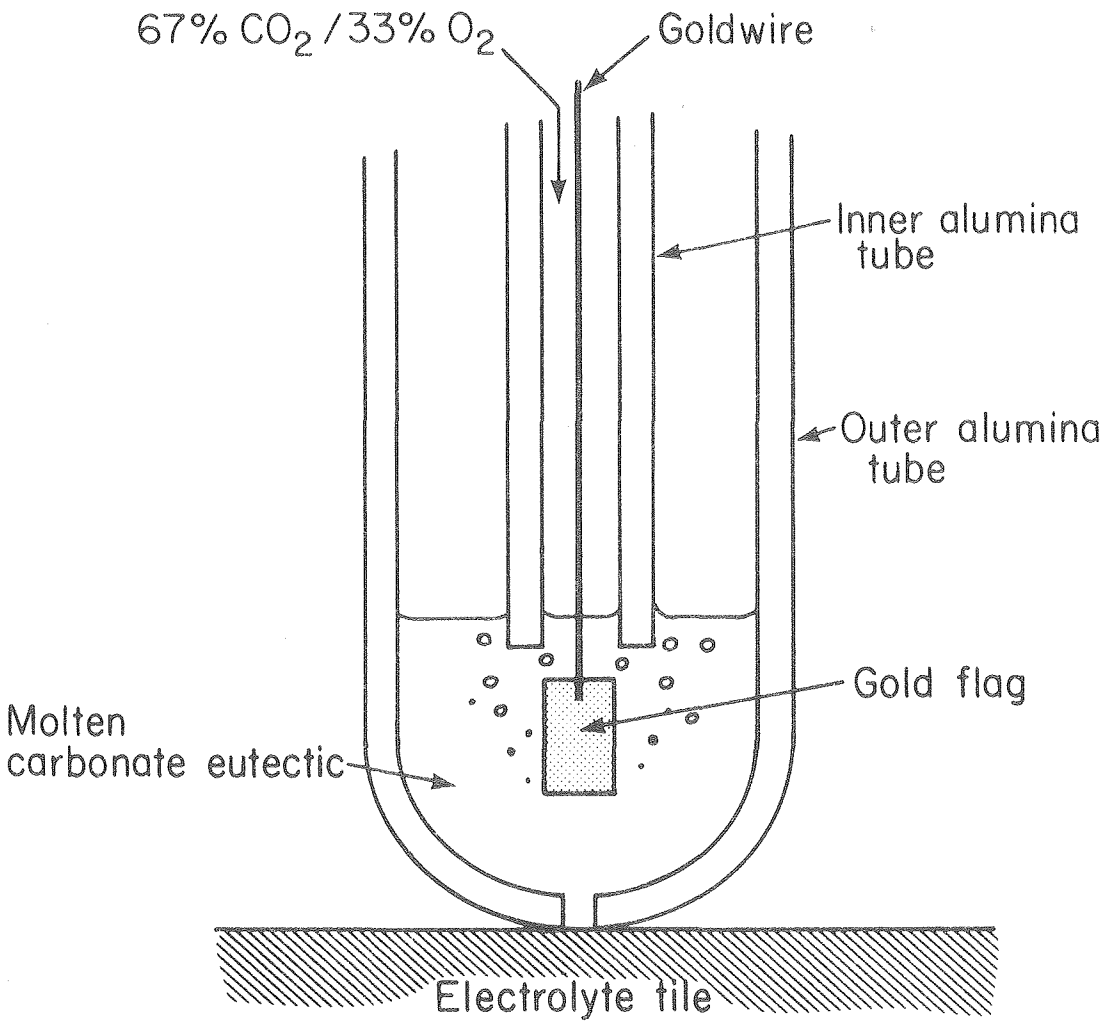

REFERENCE ELECTRODE

XBL 805-776

FIGURE 2

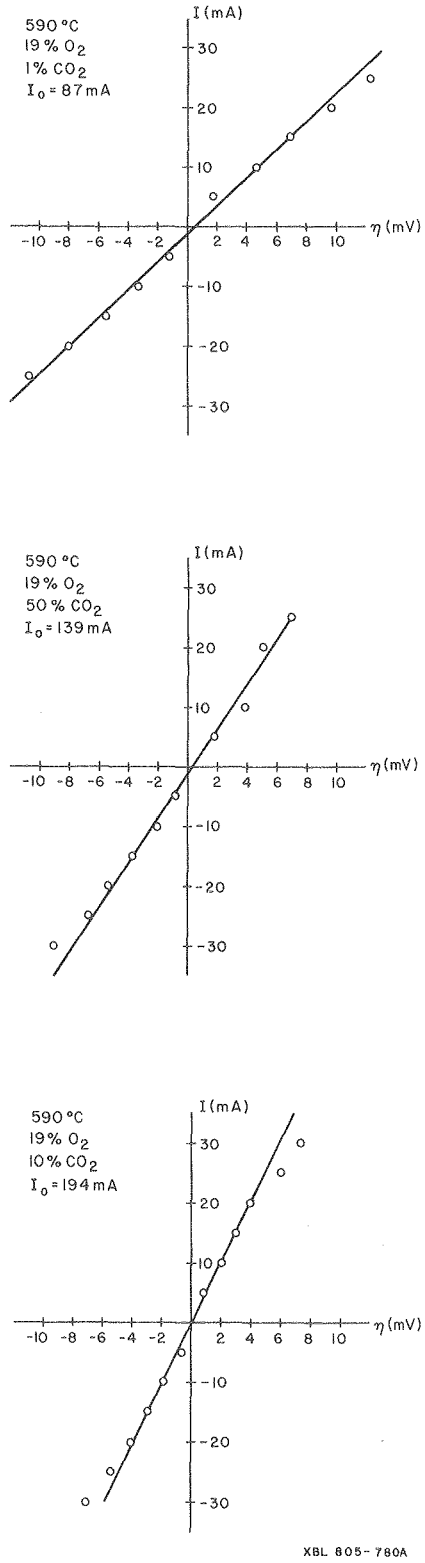
590 °C
19 % O_2
1% CO_2
I_o = 87 mA
I (mA)
30
20
10
-10
-20
-30
-10 -8 -6 -4 -2
2 4 6 8 10
η (mV)
590 °C
19 % O_2
50 % CO_2
I_o = 139 mA
I (mA)
30
20
10
-10
-20
-30
-10 -8 -6 -4 -2
2 4 6 8 10
η (mV)
590 °C
19 % O_2
10 % CO_2
I_o = 194 mA
I (mA)
30
20
10
-10
-20
-30
-10 -8 -6 -4 -2
2 4 6 8 10
η (mV)
XBL 805-780A

FIGURE 3

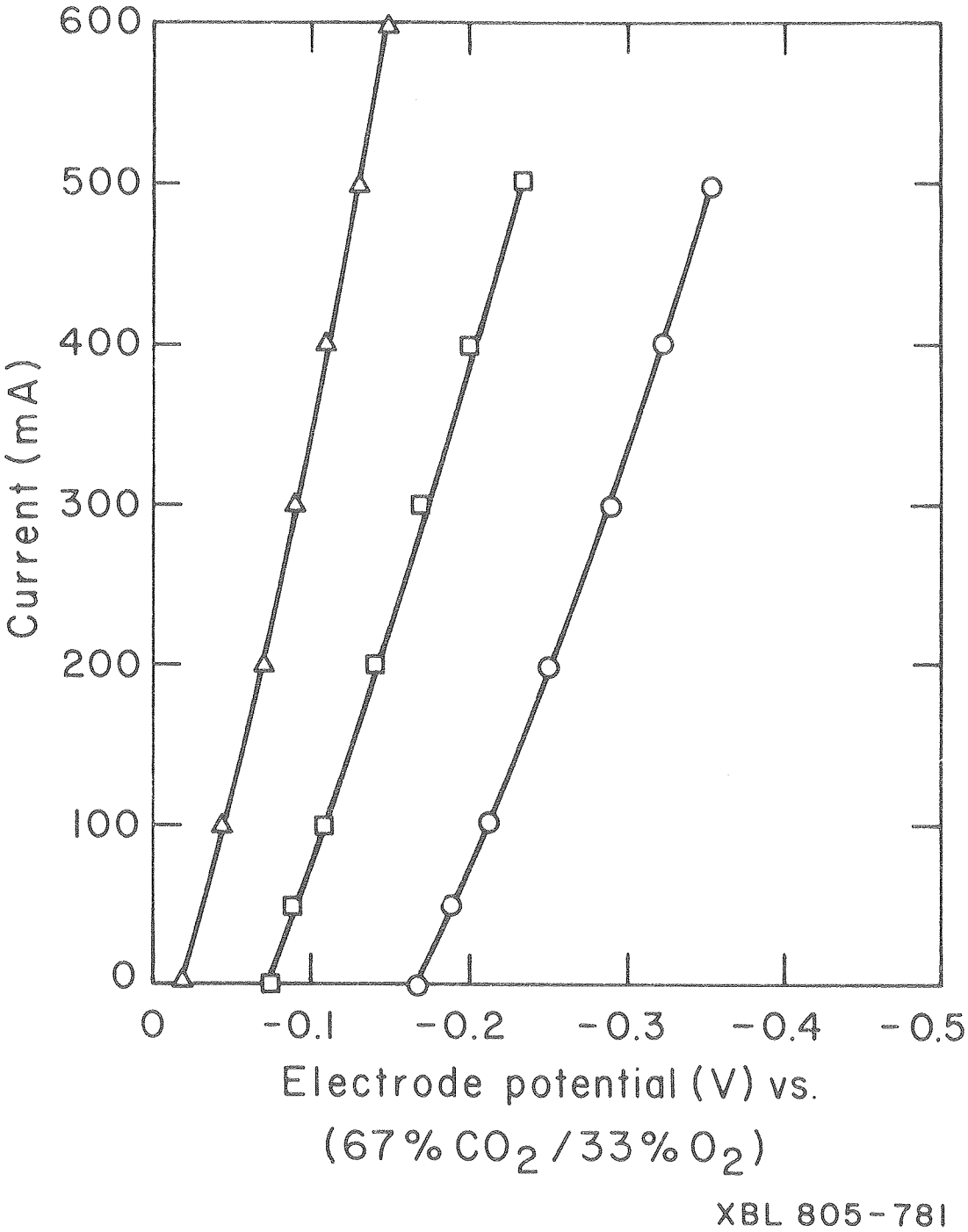

XBL 805-781

FIGURE 4

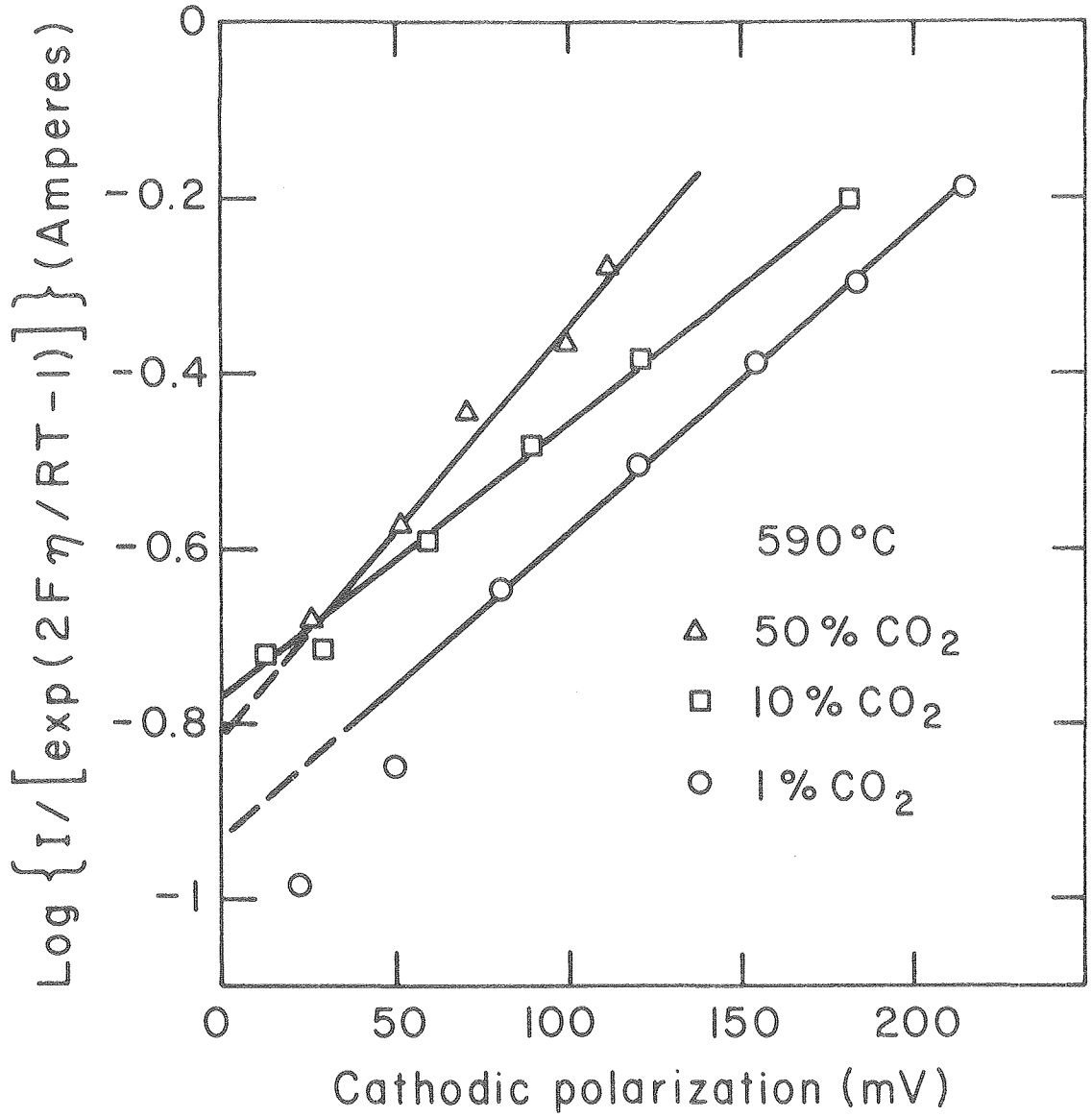

XBL 805-782

FIGURE 5

This report was done with support from the Department of Energy. Any conclusions or opinions expressed in this report represent solely those of the author(s) and not necessarily those of The Regents of the University of California, the Lawrence Berkeley Laboratory or the Department of Energy.

Reference to a company or product name does not imply approval or recommendation of the product by the University of California or the U.S. Department of Energy to the exclusion of others that may be suitable.

TECHNICAL INFORMATION DEPARTMENT
LAWRENCE BERKELEY LABORATORY
UNIVERSITY OF CALIFORNIA
BERKELEY, CALIFORNIA 94720